Expression of Antibody Fragments with a Controlled *N*-Glycosylation Pattern and Induction of Endoplasmic Reticulum-Derived Vesicles in Seeds of Arabidopsis[1][C][W][OA]

Andreas Loos, Bart Van Droogenbroeck[2], Stefan Hillmer, Josephine Grass, Martin Pabst, Alexandra Castilho, Renate Kunert, Mifang Liang, Elsa Arcalis, David G. Robinson, Ann Depicker, and Herta Steinkellner*

Department of Applied Genetics and Cell Biology (A.L., A.C., E.A., H.S.), Department of Chemistry (J.G., M.P.), and Department of Applied Microbiology (R.K.), University of Natural Resources and Applied Life Sciences, A–1190 Vienna, Austria; Department of Plant Systems Biology, Flanders Institute for Biotechnology, and Department of Plant Biotechnology and Genetics, Ghent University, B–9052 Ghent, Belgium (B.V.D., A.D.); Department of Plant Cell Biology, Centre for Organismal Studies, University of Heidelberg, D–69120 Heidelberg, Germany (S.H., D.G.R.); and State Key Laboratory for Infectious Disease Control and Prevention, National Institute for Viral Disease Control and Prevention, 100052 Beijing, People's Republic of China (M.L.)

Intracellular trafficking and subcellular deposition are critical factors influencing the accumulation and posttranslational modifications of proteins. In seeds, these processes are not yet fully understood. In this study, we set out to investigate the intracellular transport, final destination, *N*-glycosylation status, and stability of the fusion of recombinant single-chain variable fragments to the crystallizing fragment of an antibody (scFv-Fc) of two antiviral monoclonal antibodies (2G12 and HA78). The scFv-Fcs were expressed in Arabidopsis (*Arabidopsis thaliana*) seeds and leaves both as secretory molecules and tagged with an endoplasmic reticulum (ER) retention signal. We demonstrate differential proteolytic degradation of scFv-Fcs in leaves versus seeds, with higher degradation in the latter organ. In seeds, we show that secretory versions of HA78 scFv-Fcs are targeted to the extracellular space but are deposited in newly formed ER-derived vesicles upon KDEL tagging. These results are in accordance with the obtained *N*-glycosylation profiles: complex-type and ER-typical oligomannosidic *N*-glycans, respectively. HA78 scFv-Fcs, expressed in seeds of an Arabidopsis glycosylation mutant lacking plant-specific *N*-glycans, exhibit custom-made human-type *N*-glycosylation. In contrast, 2G12 scFv-Fcs carry exclusively ER-typical oligomannosidic *N*-glycans and were deposited in newly formed ER-derived vesicles irrespective of the targeting signals. HA78 scFv-Fcs exhibited efficient virus neutralization activity, while 2G12 scFv-Fcs were inactive. We demonstrate the efficient generation of scFv-Fcs with a controlled *N*-glycosylation pattern. However, our results also reveal aberrant subcellular deposition and, as a consequence, unexpected *N*-glycosylation profiles. Our attempts to elucidate intracellular protein transport in seeds contributes to a better understanding of this basic cell biological mechanism and is a step toward the versatile use of Arabidopsis seeds as an alternative expression platform for pharmaceutically relevant proteins.

Recombinant monoclonal antibodies (mAbs) are of high therapeutic potential and have thus become a major product of the pharmaceutical industry (Aggarwal, 2009). In addition to full-length mAbs, antibodies are being engineered to alter their size, pharmacokinetics, specificity, valency, effector functions, etc. in order to better suit the intended applications (for review, see Filpula, 2007; Harmsen and De Haard, 2007). Of particular interest among these engineered fragments are single-chain variable fragments (scFvs), fusions of variable heavy and variable light domains that retain an antigen-binding function. Due to their smaller size as compared with their full-length counterparts, these molecules penetrate target tissues better and can even bind to intracellular targets. Furthermore, multimerization via disulfide bonds and/or multimerization domains allows for the production of divalent or higher order antibody-like molecules, where increased avidity

[1] This work was supported by a European Union Pharma-Planta (Framework VI) Ph.D. stipend to A.L., by project L575-B13 of the Fonds zur Förderung der wissenschaftlichen Forschung, by project Nr239375 (Laura Bassi Centres of Expertise) of the Österreichische Forschungsförderungsgesellschaft mbH, as well as by the European Union Cooperation in Science and Technology Action FA0804.

[2] Present address: Institute of Agricultural and Fisheries Research, Burgemeester Van Gansberghelaan 115, 9820 Merelbeke, Belgium.

* Corresponding author; e-mail herta.steinkellner@boku.ac.at.

The author responsible for distribution of materials integral to the findings presented in this article in accordance with the policy described in the Instructions for Authors (www.plantphysiol.org) is: Herta Steinkellner (herta.steinkellner@boku.ac.at).

[C] Some figures in this article are displayed in color online but in black and white in the print edition.

[W] The online version of this article contains Web-only data.

[OA] Open Access articles can be viewed online without a subscription.

www.plantphysiol.org/cgi/doi/10.1104/pp.110.171330

has positive effects on the target-binding efficacy. Very promising products in this respect are so called scFv-Fcs (i.e. fusions of a scFv to the crystallizing fragment of an antibody [Fc; hinge-C_H2-C_H3]). These molecules spontaneously fold and dimerize to give a structure similar to a full-length IgG (Zhang et al., 2007; Cao et al., 2009). Despite their small size, Fc-mediated effector functions are maintained and finally lead to the elimination of the antigen-antibody complex from the blood stream (Powers et al., 2001). An additional benefit of such molecules is their composition: one scFv-Fc consists of two polypeptides from one gene. Thus, homodimerization but not heterotetramerization is necessary for correct folding, which could allow for more efficient expression. In general, scFv-Fcs exhibit characteristics equivalent to their parent IgG (Shu et al., 1993; Powers et al., 2001; Cao et al., 2009) and have been tested for similar applications (Li et al., 2000; Yuan et al., 2006; Mori and Kim, 2008; De Lorenzo and D'Alessio, 2009; Olafsen et al., 2009; Riccio et al., 2009).

Plant seeds are increasingly becoming an attractive alternative platform for the production of recombinant proteins. In particular, low production costs, high accumulation of recombinant proteins in the small volume of the seed, and product stability over years allows the separation of cultivation from the purification process, thereby making this system an economically feasible proposition (for review, see Boothe et al., 2010). Notably, with the model plant Arabidopsis (*Arabidopsis thaliana*), very high accumulation levels have been reported, with recombinant polypeptides even exceeding 35% of the total soluble protein, which corresponds to over 70 g of recombinant protein per kg of dry seeds (De Jaeger et al., 2002). Regulatory elements from highly expressed seed storage proteins enable these elevated accumulation levels to be reached and have already been used for the expression of a scFv-Fc (Van Droogenbroeck et al., 2007). However, the high accumulation of recombinant proteins in seeds, including mAbs and scFv-Fcs, not only depends

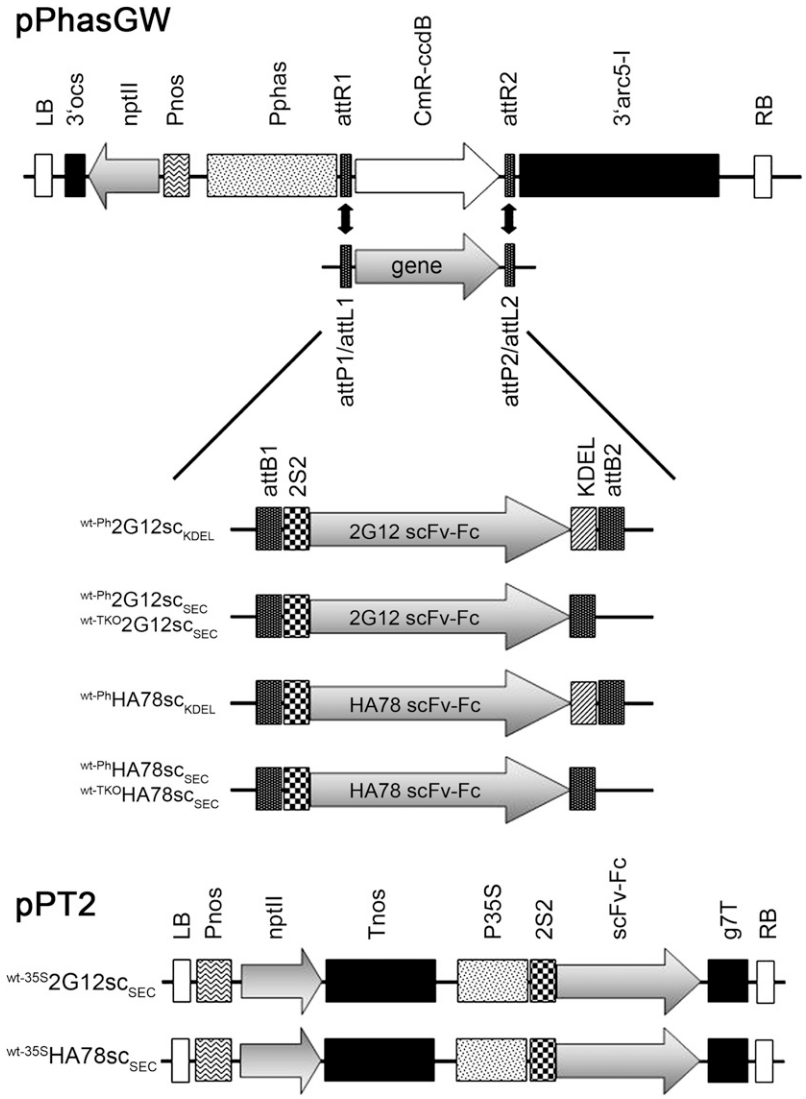

Figure 1. Schematic overview of the T-DNA region of the expression constructs generated in this study. $^{wt\text{-}Ph}$2G12sc$_{SEC}$, $^{wt\text{-}Ph}$2G12sc$_{KDEL}$, $^{wt\text{-}Ph}$HA78sc$_{SEC}$, and $^{wt\text{-}Ph}$HA78sc$_{KDEL}$ were cloned into the vector pPhasGW (F. Morandini, B. Van Droogenbroeck, and A. Depicker, unpublished data) for transformation into wild-type and TKO plants. $^{wt\text{-}35S}$2G12sc$_{SEC}$ and $^{wt\text{-}35S}$HA78sc$_{SEC}$ were additionally cloned into the binary expression vector pPT2 (Strasser et al., 2005). LB, Left border; 3′ocs, 3′ end of the octopine synthase gene; nptII, neomycin phosphotransferase II; Pnos, nopaline synthase promoter; Pphas, β-phaseolin promoter (1–1,470; GenBank accession no. J01263); attB1, attB2, attP1, attP2, attL1, attL2, attR1, and attR2, recombination sites for Gateway cloning (Invitrogen, 2003); CmR-ccdB, Gateway positive/negative selection cassette; 3′arc5-I, approximately 4,000 bp of 3′ flanking region of the arceline 5I gene (part of GenBank accession no. Z50202); RB, right border; 2S2, signal peptide of the Arabidopsis 2S2 seed storage protein (Krebbers et al., 1988); KDEL, ER retrieval motif; Tnos, nopaline synthase terminator; P35S, cauliflower mosaic virus 35S promoter; g7T, 200 bp of transcript 7 3′ region (bp 398–598, Dhaese et al., 1983).

Table I. *Overview of scFv-Fc-expressing lines*

Name	scFv-Fc Based on mAb	Targeting Signals	Expression Vector	Promoter	Genetic Background
$^{wt\text{-}Ph}2G12sc_{SEC}$	2G12	For secretion	pPhasGW	β-Phaseolin	Wild type
$^{wt\text{-}Ph}2G12sc_{KDEL}$	2G12	For ER retention	pPhasGW	β-Phaseolin	Wild type
$^{TKO\text{-}Ph}2G12sc_{SEC}$	2G12	For secretion	pPhasGW	β-Phaseolin	TKO
$^{wt\text{-}35S}2G12sc_{SEC}$	2G12	For secretion	pPT2	35S	Wild type
$^{wt\text{-}Ph}HA78sc_{SEC}$	HA78	For secretion	pPhasGW	β-Phaseolin	Wild type
$^{wt\text{-}Ph}HA78sc_{KDEL}$	HA78	For ER retention	pPhasGW	β-Phaseolin	Wild type
$^{TKO\text{-}Ph}HA78sc_{SEC}$	HA78	For secretion	pPhasGW	β-Phaseolin	TKO
$^{wt\text{-}35S}HA78sc_{SEC}$	HA78	For secretion	pPT2	35S	Wild type

upon the level of synthesis but also on their stability after deposition within a suitable compartment. In this respect, a frequently reported approach is KDEL-mediated retention within the endoplasmic reticulum (ER), which seems to allow for increased protein accumulation (Wandelt et al., 1992; Fiedler et al., 1997; Ko et al., 2005; Petruccelli et al., 2006; Laguía-Becher et al., 2010).

The deposition of recombinant proteins in a specific subcellular compartment has identified peculiarities of the seed secretory system, which obviously differs from the commonly accepted default pathway. The most obvious difference is the absence of a lytic vacuole, in terms of size of the dominant organelle of most plant cells, and instead the presence of protein storage vacuoles (PSVs), where the endogenous seed storage proteins are deposited (for review, see Müntz, 1998; Robinson et al., 2005). However, the targeting of recombinant proteins in seeds is not yet fully understood. For example, KDEL-tagged as well as secretory proteins have been detected in protein storage vacuoles, in the cell wall, in ER-derived compartments, or in a combination of the three (Herman et al., 1990; Philip et al., 1998, 2001; Wright et al., 2001; Reggi et al., 2005; Downing et al., 2006; Petruccelli et al., 2006; Van Droogenbroeck et al., 2007; Abranches et al., 2008; Schmidt and Herman, 2008; Loos et al., 2011). As a consequence of this atypical targeting and deposition, seed-derived recombinant products may carry unusual *N*-glycosylation profiles (Van Droogenbroeck et al., 2007; Rademacher et al., 2008; Ramessar et al., 2008). Since the glycosylation status of many therapeutic proteins, including mAbs and scFv-Fcs, has a profound effect on their biological activity, it is of great importance to fully understand the molecular mechanisms that underlie targeting along the secretory pathway and final deposition.

In this study, we set out to explore further the potential of plant seeds as a versatile expression platform for valuable recombinant proteins. To this end, a series of scFv-Fc versions of the two antiviral mAbs 2G12 and HA78 were placed under the control of seed-specific regulatory sequences. Secretory as well as KDEL-tagged versions were used to transform Arabidopsis wild-type plants as well as a glycosylation mutant lacking plant-specific *N*-glycosylation (Strasser et al., 2004). For comparison, some of these constructs were additionally placed under the control of the constitutive cauliflower mosaic virus 35S promoter. Expression levels and the stability of seed- and leaf-produced recombinant scFv-Fcs were determined using ELISA and immunoblotting. *N*-Glycosylation profiles of the different scFv-Fc variants were determined by mass spectrometry, and the actual subcellular localization of the seed-produced scFv-Fcs was demonstrated by immunogold electron microscopy (IEM). Finally, functional activities of the scFv-Fc variants were determined by antigen-binding and virus neutralization assays.

RESULTS

Cloning and Plant Transformation

Secretory and KDEL-tagged scFv-Fc versions of two different model antibodies (2G12 against *Human immunodeficiency virus* [HIV] and HA78 against *Hepatitis A virus*; Trkola et al., 1996; Cao et al., 2008) were constructed and cloned into the pPhasGW destination

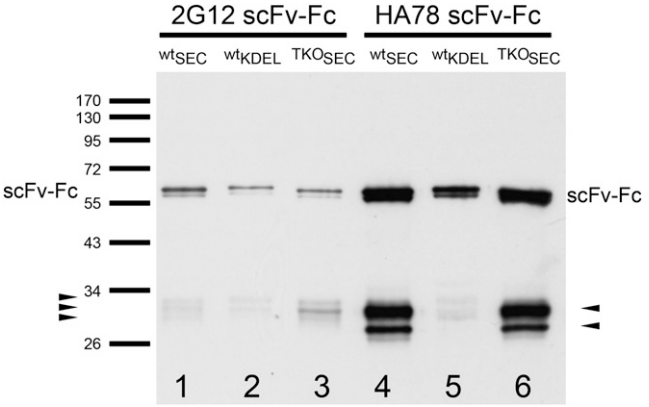

Figure 2. Immunodetection of β-phaseolin-driven scFv-Fcs extracted from seeds. One microliter of crude seed extracts (corresponding to 10 μg of seeds) was separated by SDS-PAGE, blotted on a nitrocellulose membrane, and the scFv-Fcs were detected with goat anti-human IgG (H+L) HRP conjugate (Promega; W403B) and a chemiluminescent substrate (SuperSignal West Pico Chemiluminescent Substrate; Pierce). After 3 s of film exposure, all constructs could be visualized. Arrowheads indicate degradation fragments, and bars indicate the height of marker bands (in kD).

Table II. *Maximal expression levels of scFv-Fcs in Arabidopsis seeds*

n.d., Not determined.

Name	Primary Transformants Screened	Maximum Expression Level
		μg mg^{-1} dry seeds
$^{wt\text{-}Ph}$2G12sc$_{SEC}$	43	0.8
$^{wt\text{-}Ph}$2G12sc$_{KDEL}$	40	0.8
$^{TKO\text{-}Ph}$2G12sc$_{SEC}$	25	3.5
$^{wt\text{-}35S}$2G12sc$_{SEC}$		n.d.
$^{wt\text{-}Ph}$HA78sc$_{SEC}$	30	8.0
$^{wt\text{-}Ph}$HA78sc$_{KDEL}$	40	3.9
$^{TKO\text{-}Ph}$HA78sc$_{SEC}$	40	9.4
$^{wt\text{-}35S}$HA78sc$_{SEC}$		n.d.

vector (F. Morandini, B. Van Droogenbroeck, and A. Depicker, unpublished data; Fig. 1) and were expressed under the control of the seed-specific β-phaseolin promoter from *Phaseolus vulgaris* (De Jaeger et al., 2002; Van Droogenbroeck et al., 2007). The vectors were used to transform Arabidopsis Columbia wild-type (wt) plants and glycosylation mutants lacking plant-specific core α-1,3-fucosylation and β-1,2-xylosylation, referred to as "triple knockout" (TKO; Strasser et al., 2004). In addition, the secretory versions were fused to the constitutive cauliflower mosaic virus 35S promoter in the vector pPT2 (Strasser et al., 2005) and used to transform Arabidopsis wild-type plants. In total, eight different combinations of construct and genetic background were established (Table I).

Expression of scFv-Fc Molecules

At least 25 primary transformants of each series of transformants were screened by ELISA and immunoblotting (Fig. 2; Table II). Based on expression levels, two lines each were selected and selfed to obtain homozygous plants. Maximal expression levels as determined by ELISA ranged from 0.8 to 9.4 mg recombinant protein g^{-1} dry seed weight (Table II). Generally, the HA78 constructs accumulated to a higher level than the 2G12 constructs and KDEL tagging did not lead to an increased accumulation. These results are in accordance with the recently expressed full-length versions of 2G12 and HA78 mAbs in Arabidopsis seeds (Loos et al., 2011). Expression levels of the 35S-driven constructs were not analyzed in detail. However, when compared with the β-phaseolin-driven constructs, they were significantly lower (as deduced from immunoblotting).

Seed extracts from transformed plants were subjected to immunoblotting and revealed strong signals consisting of double bands at approximately 60 kD (Fig. 2). The smaller, less intense band represents the nonglycosylated fraction, as previously shown by Van Droogenbroeck et al. (2007). Additionally, degradation products are visible at around 28 to 34 kD. These fragments are derived from heavy chain domains as determined by mass spectrometry (MS) analysis of tryptic peptides (data not shown). KDEL-tagged versions exhibited a slightly increased mass of the intact molecule as well as of their approximately 30-kD degradation products (Fig. 2), most likely due to the KDEL tag and a different *N*-glycosylation pattern. Although the KDEL tag does not lead to an increased accumulation of scFv-Fcs, it seems to confer enhanced stability, which is especially pronounced for the HA78 scFv-Fcs (Fig. 2). The degradation pattern of the 35S-driven constructs ($^{wt\text{-}35S}$2G12sc$_{SEC}$ and $^{wt\text{-}35S}$HA78sc$_{SEC}$) extracted from leaves clearly differs from the degradation pattern of the scFv-Fcs extracted from seeds (Figs. 2 and 3), indicating the presence of different proteases in these two tissues. Surprisingly, 35S-driven scFv-Fcs ($^{wt\text{-}35S}$2G12sc$_{SEC}$ and $^{wt\text{-}35S}$HA78sc$_{SEC}$) accumulated a higher proportion of intact protein in leaves than in seeds (Figs. 2 and 3; Supplemental Fig. S5).

N-Glycosylation

All constructs carry one *N*-glycosylation site in the C_H2 domain. The *N*-glycosylation status of Protein A-purified scFv-Fcs was analyzed by liquid-chromatography (LC)-MS (Fig. 4). KDEL-tagged versions of 2G12 and HA78 ($^{wt\text{-}Ph}$HA78sc$_{KDEL}$ and $^{wt\text{-}Ph}$2G12sc$_{KDEL}$) exhibited as expected exclusively oligomannosidic structures, mainly Man7 and Man8. Seed-produced secretory HA78 constructs ($^{wt\text{-}Ph}$HA78sc$_{SEC}$ and $^{TKO\text{-}Ph}$HA78sc$_{SEC}$) carry complex-type glycans, GnGnXF and GnGn, respectively, depending on the expression host, Columbia wild type or TKO. In addition, substantial amounts of oligomannosidic structures are present. This ER-typical glycosylation is completely absent when secretory HA78 is expressed in leaves:

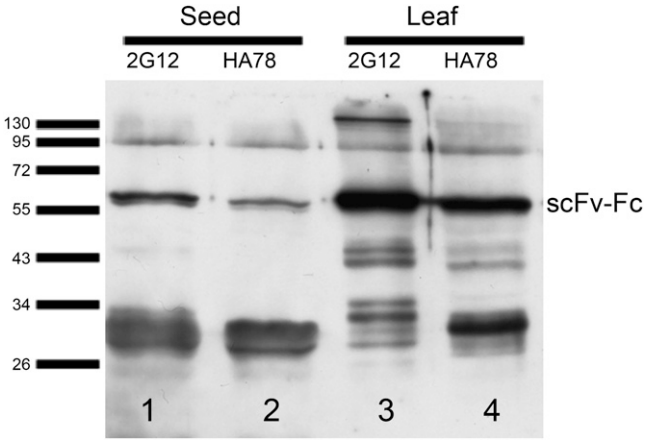

Figure 3. Immunodetection of 35S-driven scFv-Fcs extracted from seeds and leaves. Nine microliters of crude seed extract and 5 μL of crude leaf extract (corresponding to 90 μg of seeds and 375 μg of leaf material) were separated by SDS-PAGE, blotted on a nitrocellulose membrane, and detected with goat anti-human IgG (H+L) HRP conjugate (Promega; W403B) and a chemiluminescent substrate (Super-Signal West Pico Chemiluminescent Substrate; Pierce). Film exposure for 30 s reveals scFv-Fc bands as well as degradation products. Bars indicate the height of marker bands (in kD).

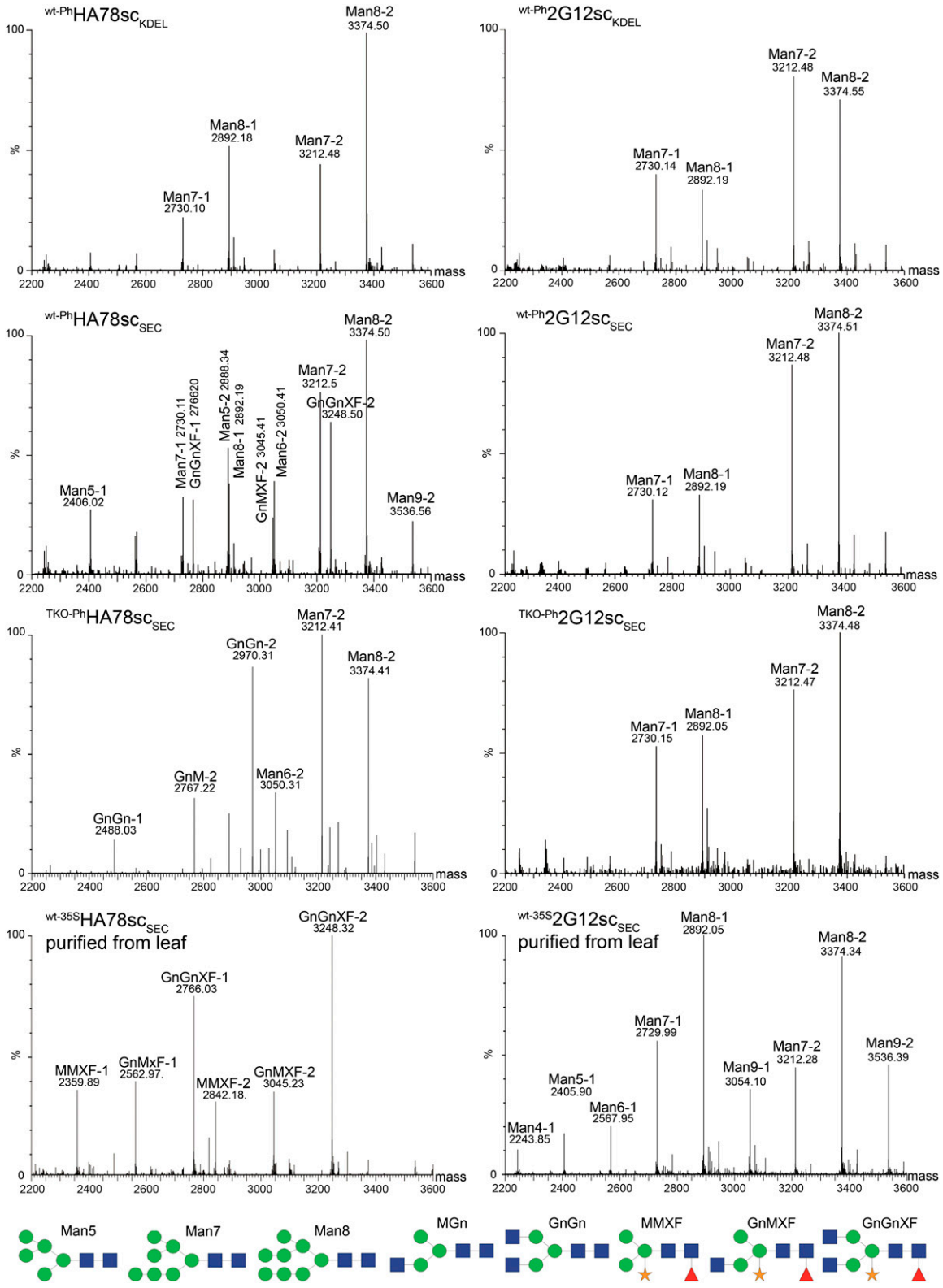

Figure 4. *N*-Glycosylation patterns of different seed- and leaf-produced scFv-Fcs. *N*-Glycan analysis was carried out by LS-ESI-MS of tryptic peptides. Due to incomplete tryptic digest, each glycan structure is represented by two glycopeptides assigned -1 and -2. All 2G12 constructs as well as $^{wt\text{-}Ph}HA78sc_{KDEL}$ carry exclusively oligomannosidic *N*-glycans. $^{wt\text{-}Ph}HA78sc_{SEC}$ carries xylosylated and fucosylated complex-type *N*-glycans as well as oligomannosidic structures, while $^{TKO\text{-}Ph}HA78sc_{SEC}$ carries nonxylosylated and nonfucosylated complex-type *N*-glycans as well as oligomannosidic structures. $^{wt\text{-}35S}HA78sc_{SEC}$ extracted from leaves carries xylosylated and fucosylated complex-type *N*-glycans. The depicted glycoforms show one of the possible isoforms. For *N*-glycan nomenclature, see www.proglycan.com [See online article for color version of this figure.]

$^{wt\text{-}35S}$HA78sc$_{SEC}$ extracted from leaves exhibits exclusively complex-type *N*-glycans, with GnGnXF as the single dominant structure. Surprisingly, all 2G12 constructs, irrespective of their targeting information or their regulatory sequences ($^{wt\text{-}Ph}$2G12sc$_{SEC}$, $^{wt\text{-}Ph}$2G12sc$_{KDEL}$, $^{TKO\text{-}Ph}$2G12sc$_{SEC}$, and $^{wt\text{-}35S}$2G12sc$_{SEC}$ extracted from leaf), carry exclusively oligomannosidic *N*-glycans.

The 35S-driven constructs accumulated only at a low level in seeds (Fig. 3). Thus, it was not possible to purify sufficient amounts of 35S-driven scFv-Fc from this tissue to proceed to *N*-glycan analysis. However, the *N*-glycan analysis of HA78 degradation fragments revealed the presence of complex (GnGnXF) and oligomannosidic structures (Supplemental Figs. S5 and S6; Supplemental Results S1). Interestingly, small amounts of single GlcNAc stubs were found as well. These single GlcNAc stubs have not been found on any of our seed- or leaf-produced scFv-Fcs and mAbs (Loos et al., 2011) but are known from other systems (Islam et al., 1991; Zeng et al., 2003; Rademacher et al., 2008; Ramessar et al., 2008; Floss et al., 2009).

Man7 Isomer Distribution

Another interesting observation was the presence of a relatively high proportion of Man7 structures in seed-extracted scFv-Fcs, even in constructs designed for secretion (i.e. $^{wt\text{-}Ph}$HA78sc$_{SEC}$, $^{TKO\text{-}Ph}$HA78sc$_{SEC}$, $^{wt\text{-}Ph}$2G12sc$_{SEC}$, and $^{TKO\text{-}Ph}$2G12sc$_{SEC}$). As known from other studies, this Man7 structure occurs in at least three isomers, Man7.1, Man7.2, and Man7.7 (Neeser et al., 1985; Tomiya et al., 1991). There is some evidence that Man7.1 isomers are substrates for the endoplasmic reticulum-associated protein degradation (ERAD) pathway, which directs misfolded proteins from the ER for ubiquitination and subsequent proteasomal degradation (Clerc et al., 2009). We set out to analyze the Man7 isomer composition of scFv-Fcs in more detail (Fig. 5). In fact, $^{wt\text{-}Ph}$HA78sc$_{SEC}$ and $^{TKO\text{-}Ph}$HA78sc$_{SEC}$ had the lowest proportion of Man7.1 (approximately 30% of the Man7 glycans and approximately 8% of the oligomannosidic fraction). The ER-retained $^{wt\text{-}Ph}$HA78sc$_{KDEL}$ contains clearly more Man7.1 (approximately 62% of the Man7 glycans and approximately 13% of the oligomannosidic fraction), while $^{wt\text{-}Ph}$2G12sc$_{SEC}$ shows the highest amount (approximately 90% of the Man7 glycans and 26% of the oligomannosidic fraction).

Subcellular Localization

In order to reveal the stations of intracellular transport and the final destination of the recombinant scFv-Fcs, IEM was carried out on mature and developing seeds. The final deposition status of the target proteins can be determined in mature seeds; however, more organelles are visible in developing seeds, therefore enabling a more detailed investigation of intracellular trafficking. Plants that were transformed with scFv-Fcs driven by the seed-specific phaseolin promoters (i.e. $^{wt\text{-}Ph}$2G12sc$_{SEC}$, $^{wt\text{-}Ph}$2G12sc$_{KDEL}$, $^{wt\text{-}Ph}$HA78sc$_{SEC}$, and $^{wt\text{-}Ph}$HA78sc$_{KDEL}$) were analyzed. The results for mature seeds are shown in Supplemental Figures S1 to S4 and in Supplemental Results S1.

Intense labeling of the extracellular space was obtained in seeds expressing $^{wt\text{-}Ph}$HA78sc$_{SEC}$, showing the efficient secretion of the scFv-Fc to that compartment (Fig. 6A). In addition, dense vesicles were intensely labeled (Fig. 6B), but minor amounts of gold particles were also detected in the Golgi stack itself (Fig. 6C). This labeling pattern is reminiscent of the expression of the secretory full-length antibody versions of 2G12 and HA78 in Arabidopsis seeds, which also localize to the same structures (Loos et al., 2011). $^{wt\text{-}Ph}$HA78sc$_{KDEL}$ accumulated in globular, membrane-delimited structures of around 200 to 400 nm diameter (Fig. 7). These structures were partially studded with ribosomes, indicating their ER origin, and are thus called endoplasmic reticulum-derived vesicles (ERVs). The PSVs were consistently only slightly labeled (Fig. 7C). However, none of the other compartments, like the Golgi apparatus (Fig. 7A), putative multivesicular bodies (Fig. 7B), or the extracellular space (data not shown), was labeled. Mature seeds expressing $^{wt\text{-}Ph}$HA78sc$_{SEC}$ also showed gold particles in the extracellular space; however, in contrast to developing seeds, ERVs were additionally present in the cytoplasm and labeled (Supplemental Fig. S1). Mature seeds expressing $^{wt\text{-}Ph}$HA78sc$_{KDEL}$ exhibited labeling exclusively in ERVs and dilated nuclear envelope (Supplemental Fig. S2).

Surprisingly, IEM studies in developing seeds expressing $^{wt\text{-}Ph}$2G12sc$_{SEC}$ (Fig. 8) exhibited a similar labeling pattern as obtained for $^{wt\text{-}Ph}$HA78sc$_{KDEL}$ (Fig. 7). Gold label was found exclusively in globular, partly ribosome-studded ER-derived vesicles of around 200 to 400 nm. In addition, the nuclear envelope was partially dilated and labeled (Fig. 8A), which was not observed for the HA78 scFv-Fc constructs. Golgi stacks, the extracellular space, as well as the PSV were devoid of label (Fig. 8, B, D, and E). Such an unexpected labeling pattern was also detected in mature seeds (Supplemental Fig. S3). These findings were surprising, as the protein was designed for secretion; however, they were consistent with the observed ER-typical oligomannosidic *N*-glycan profile. For $^{wt\text{-}Ph}$2G12sc$_{KDEL}$, IEM was conducted on mature seeds only (Supplemental Fig. S4) and gave a very similar result as for $^{wt\text{-}Ph}$2G12sc$_{SEC}$, with intensive labeling of ERVs. Notably, ERVs were not detected in nontransformed Arabidopsis seeds (data not shown).

Antigen-Binding Activity and in Vitro Virus Neutralization

Functional activities of seed-produced scFv-Fcs were also determined. First, the antigen-binding capacities of purified $^{wt\text{-}Ph}$2G12sc$_{KDEL}$, $^{wt\text{-}Ph}$HA78sc$_{SEC}$, $^{wt\text{-}Ph}$HA78sc$_{KDEL}$, as well as $^{TKO\text{-}Ph}$HA78sc$_{SEC}$ were determined by ELISA. Whereas all HA78 scFv-Fc variants

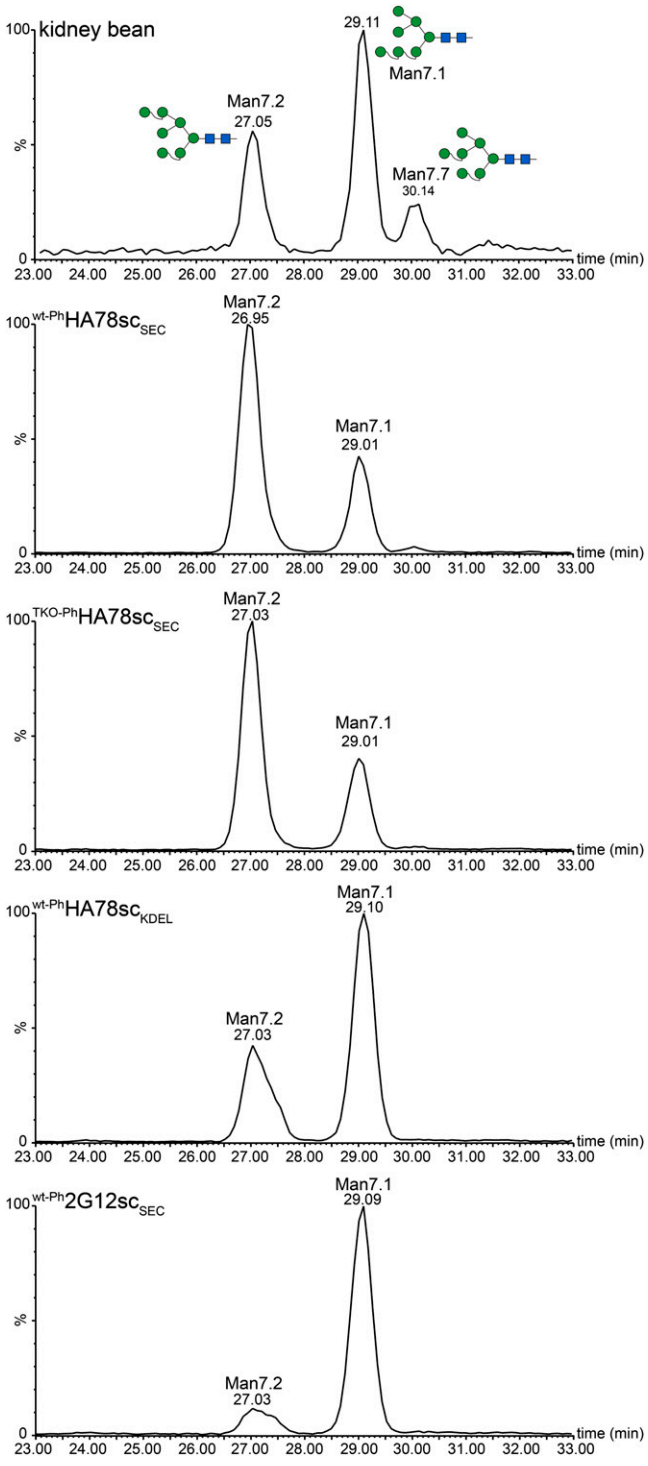

Figure 5. Man7 isomer analysis. Man7 *N*-glycans of SDS-PAGE-separated, Protein A-purified scFv-Fcs were released, separated by a capillary porous graphitic carbon column, and detected by LC-ESI-MS. Reference glycans were prepared from *P. vulgaris* (kidney bean) in a similar manner. In the secretory HA78 constructs, the Man7.1 isoform is predominant, whereas in $^{wt\text{-}Ph}$HA78sc$_{KDEL}$ and $^{wt\text{-}Ph}$2G12sc$_{SEC}$, the Man7.2 isoform is prevalent. [See online article for color version of this figure.]

exhibited binding comparable to a Chinese hamster ovary (CHO)-produced full-length mAb (Fig. 9), none of the 2G12 constructs was able to bind the respective antigen (data not shown). In vitro virus neutralization assays were conducted with the same scFv-Fcs. Again, the three HA78 scFv-Fc variants exhibited a hepatitis A virus neutralization efficiency similar to CHO- and plant-produced full-length mAbs (Table III), while $^{wt\text{-}Ph}$2G12sc$_{KDEL}$ did not show any neutralizing activity (Table IV).

DISCUSSION

In this study, we focused on the expression, stability, intracellular trafficking, deposition pattern, and *N*-glycosylation status of recombinantly expressed scFv-Fc versions of two antiviral antibodies. We have exploited the capability of plant seeds to produce high amounts of these complex, potentially therapeutic proteins. The accumulation levels of the scFv-Fcs expressed in Arabidopsis seeds lie between 0.8 and 9.4 μg mg^{-1} dry seeds (Table II). This is in the same range as recently published for the respective full-length IgGs (Loos et al., 2011) but clearly lower than previously reported for scFvs and scFv-Fcs (74 μg mg^{-1} dry seeds [De Jaeger et al., 2002] and 26 μg mg^{-1} dry seeds [Van Droogenbroeck et al., 2007], respectively). The reason for the lower accumulation level

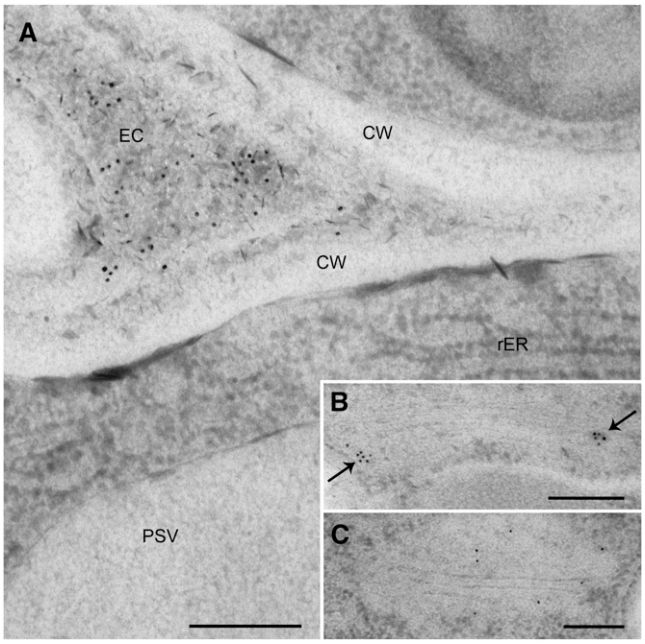

Figure 6. Subcellular localization of $^{wt\text{-}Ph}$HA78sc$_{SEC}$ in developing Arabidopsis seeds by IEM. A, Gold label was mainly found in the extracellular space. B and C, Label was also found in association with the Golgi apparatus. B, The marginal rims/attached dense vesicles and vesicles budding from the Golgi are labeled (arrows). C, Label was also found in more central parts of the Golgi apparatus. CW, Cell wall; EC, extracellular space; rER, rough ER. Bars = 200 nm.

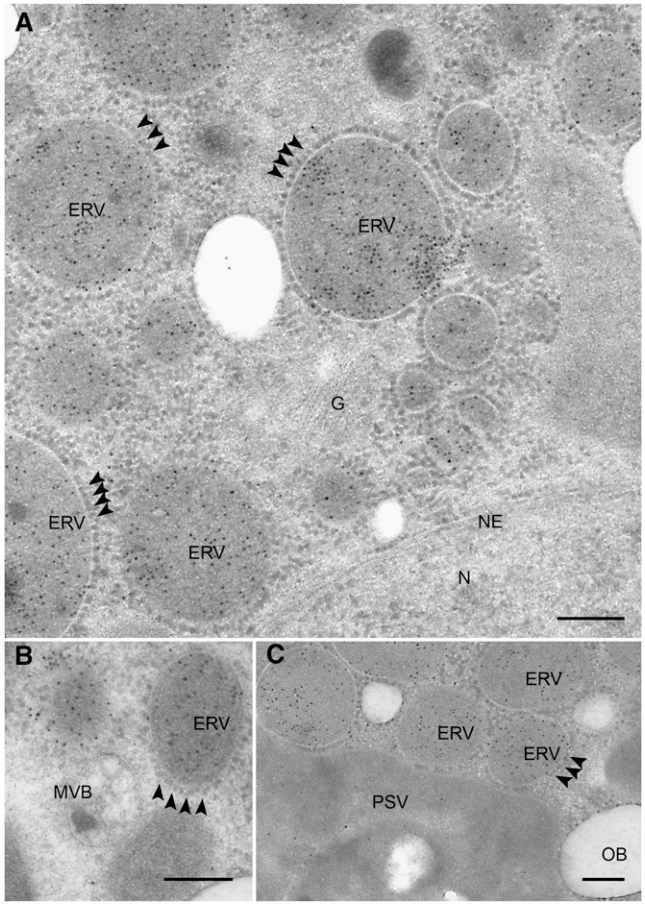

Figure 7. Subcellular localization of $^{wt\text{-}Ph}HA78sc_{KDEL}$ in developing Arabidopsis seeds by IEM. A, Gold label was nearly exclusively found in globular structures that were partially ribosome studded (arrowheads), indicating an ER origin (ERVs). The nuclear envelope was neither swollen nor labeled. B, A putative multivesicular body was not labeled. C, ER-derived globular structures were strongly labeled, the PSV was slightly labeled, and oil bodies were free of labeling. N, Nucleus; NE, nuclear envelope; MVB, multivesicular body; OB, oil body. Bars = 200 nm.

is not clear but may lie in sequence elements with unfavorable codon usage. Thus, codon optimization might further increase expression levels, as has been frequently shown (e.g. Geyer et al., 2010).

Besides the intact protein, secretory versions of both 2G12 and HA78 scFv-Fcs exhibit a substantial amount of degradation products. This degraded fraction is more pronounced for the scFv-Fc constructs than for the recently reported respective IgGs (Loos et al., 2011), indicating a reduced stability of the engineered scFv-Fc compared with the full-length counterparts. Surprisingly, seed-produced scFv-Fcs seem to be more stable when expressed to a higher level: under the control of the stronger, seed-specific β-phaseolin promoter, the ratio of intact protein to degraded peptides is higher than for the 35S-driven constructs (compare the ratio of intact scFv-Fcs versus degraded polypeptides in Fig. 2, lane 4, and Fig. 3, lane 2). One possible explanation is that proteases responsible for degradation are overloaded by the vast amount of scFv-Fc produced by the β-phaseolin promoter but still cope with the smaller amount produced by the 35S promoter. Alternatively, a different temporal and spatial control of expression might be responsible for the observed differences in degradation (Takaiwa et al., 1995).

When comparing seed- and leaf-produced scFv-Fcs, a clear difference in the degradation pattern is visible (Figs. 2 and 3). This indicates that a different set of proteases is active in the different tissues or might represent differences in the secretory pathways of these two tissues. The higher ratio of intact scFv-Fcs versus degraded peptides in leaves compared with seeds suggests that 35S-driven scFv-Fcs are more stable in leaves (Fig. 3). This contrasts with the prevailing notion that seeds possess a lower lytic potential and are thus especially well suited for recombinant protein production (Fiedler and Conrad, 1995; Stoger et al., 2002). An alternative suggestion to increase the protein stability is retention in the ER via a

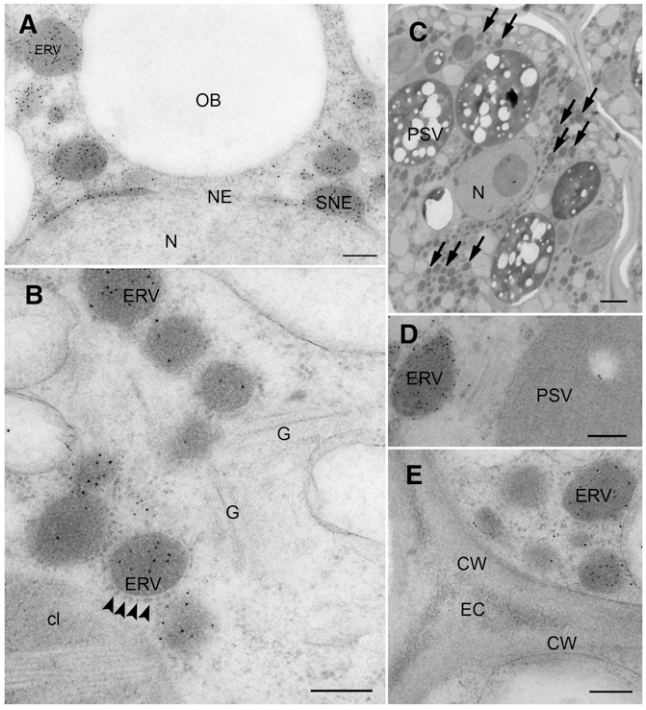

Figure 8. Subcellular localization of $^{wt\text{-}Ph}2G12sc_{SEC}$ in developing Arabidopsis seeds by IEM. A, Gold label was mainly found in ERVs. The nuclear envelope was partially swollen and labeled in a density similar to the ERVs. B, The ERVs were partially ribosome studded (arrowheads), indicating ER origin. Gold label was not found in the Golgi apparatus. C, ERVs were abundant structures. Some ERVs are indicated by arrows. D, The PSV was not labeled, but a Golgi stack was slightly labeled. E, The extracellular space was devoid of labeling. cl, Chloroplast; CW, cell wall; EC, extracellular space; G, Golgi apparatus; N, nucleus; NE, nuclear envelope; OB, oil body; SNE, swollen nuclear envelope. Bars = 200 nm (A, B, D, and E) and 1,000 nm (C).

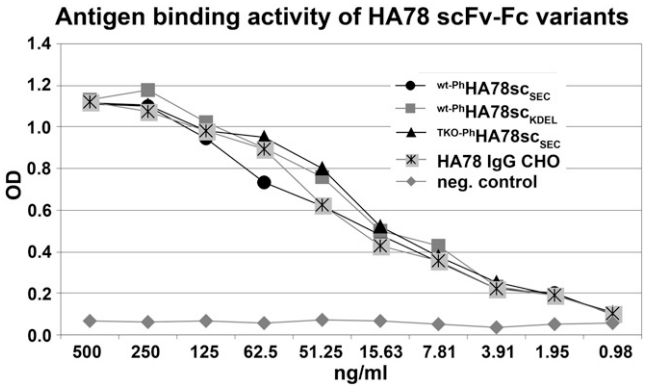

Figure 9. Antigen-binding activity of the seed-produced HA78 scFv-Fc variants. All seed-produced HA78 scFv-Fc variants exhibit the same antigen-binding activity as a CHO-produced full-length HA78 IgG. OD, Optical density.

C-terminal KDEL tag, which has also been reported to additionally increase the accumulation level (Wandelt et al., 1992; Schouten et al., 1996; Fiedler et al., 1997; Ko et al., 2005; Petruccelli et al., 2006; Laguía-Becher et al., 2010). In our study, the addition of a KDEL tag increased the stability of the protein (especially for the HA78 constructs); however, the accumulation level actually decreased. Our observations suggest that KDEL tagging is not a general technique to increase the accumulation level of recombinant proteins in Arabidopsis seeds. Moreover, the ER-typical oligomannosidic *N*-glycans on potential pharmaceutical products are only in rare cases appropriate structures (Raju, 2008).

The investigation of *N*-glycosylation status in combination with the subcellular localization of the recombinant proteins revealed some unexpected outcomes. Seed-expressed 2G12 scFv-Fcs accumulated virtually exclusively in newly formed globular structures, irrespective of their targeting signals. As ribosomes are attached to the delimiting membranes of these newly formed structures, it is anticipated that they are ERVs. This assumption is corroborated by the ER-typical oligomannosidic *N*-glycosylation pattern of the 2G12 scFv-Fcs. The formation of such ER-derived structures in dicot seeds has been suggested by others (Moravec et al., 2007; Van Droogenbroeck et al., 2007; Schmidt and Herman, 2008; Floss et al., 2009); however, the presented data did not allow drawing an unequivocal conclusion on the origin of these structures.

Particularly, the deposition of the secretory 2G12 scFv-Fcs in ERVs came as a surprise, since it was designed for secretion and thus expected to localize to the extracellular space, as reported for the full-length version of the same antibodies expressed in seeds (Loos et al., 2011). Notably, also the secretory version of 2G12 scFv-Fc expressed in leaves carries ER-typical oligomannosidic *N*-glycans instead of the expected complex-type *N*-glycosylation, indicating retention and not secretion. The reasons for this unusual subcellular deposition are not clear yet but could be due to improper folding. The complete absence of antigen-binding and virus-neutralization activity indicates an improper conformation of the polypeptide. A detailed structural analysis of 2G12 IgG had revealed an unusual conformation of this antibody (Calarese et al., 2003), with the V_H domain of one heavy chain pairing with the V_L domain of the opposing light chain. We hypothesize that the correct three-dimensional assembly of this unusual structure is impeded in the scFv-Fc, leading to the observed findings. The 2G12 scFv-Fcs seem to be recognized by the ER-based quality-control systems, and their passage farther down the secretory pathway is prevented. The increased presence of Man7.1 on 2G12 scFv-Fcs further corroborates our hypothesis, as this isoform has been reported to act as a signal for ERAD, an intracellular control mechanism for the elimination of incorrectly folded proteins (Clerc et al., 2009; Liebminger et al., 2010). In contrast, Man7 of secretory HA78 scFv-Fcs consists mainly of the Man7.2 isomer, which does not seem to be involved in the ERAD pathway (Clerc et al., 2009). Surprisingly, also the KDEL-tagged HA78 scFv-Fc has an elevated fraction of Man7.1 isomers. Thus, it seems unlikely that Man7.1 structures alone are a mandatory signal for ERAD in Arabidopsis.

KDEL-tagged HA78 scFv-Fc was detected in newly formed ER-derived vesicles. This deposition pattern is in accordance with the *N*-glycosylation pattern. However, it is not in full agreement with a similar KDEL-tagged HA78 scFv-Fc construct, which was previously expressed in Arabidopsis seeds and had accumulated to a large extent in the periplasmic space between the plasma membrane and the cell wall (Van Droogenbroeck et al., 2007). Such a periplasmic space was not detected in this study. Yet, another subcellular localization was found for a KDEL-tagged full-length version of 2G12 recently expressed in Arabidopsis seeds. This protein was targeted nearly exclusively to protein storage vacuoles, and neither formation of ERVs nor a periplasmic space was detected (Loos et al., 2011). The factors responsible for the different deposition patterns of these related KDEL-tagged polypeptides are

Table III. *In vitro virus neutralization activity of seed-produced HA78 scFv-Fcs*

In vitro virus neutralization efficiencies of the plant-produced HA78 scFv-Fcs as well as of a CHO-produced HA78 mAb are all in the same range and thereby similar to previously reported seed-produced HA78 mAbs and a scFv-Fc (Van Droogenbroeck et al., 2007; Loos et al., 2011). As a negative control, a recombinant human antibody against *Hantavirus* was used.

Sample	IC_{50}
HA78 IgG CHO	15.51
HA78 IgG plant	13.70
$^{wt\text{-}Ph}HA78sc_{SEC}$	15.95
$^{TKO\text{-}Ph}HA78sc_{SEC}$	17.22
$^{wt\text{-}Ph}HA78sc_{KDEL}$	14.51
Negative control	>50

Table IV. *In vitro virus neutralization activity of $^{wt\text{-}Ph}$2G12sc$_{SEC}$ and plant-produced full-length 2G12*

In contrast to CHO- and seed-produced 2G12 IgG (Loos et al., 2011), the seed-produced scFv-Fc does not show in vitro neutralization activity.

Sample	IC_{50}
2G12 IgG CHO	3.15
2G12 IgG plant	0.26
$^{wt\text{-}Ph}$2G12sc$_{SEC}$	>20
Negative control	>50

so far unknown. Possible reasons could be differences in the protein sequences and/or differences in expression level. However, despite their different subcellular depositions (between plasma membrane and cell wall, in ERVs, and PSVs), all these KDEL-tagged proteins carry comparable oligomannosidic *N*-glycosylation profiles, indicating identical trafficking routes along the early secretory pathway.

In contrast to the 2G12 constructs, the secretory versions of HA78 scFv-Fcs ($^{wt\text{-}Ph}$HA78sc$_{SEC}$, $^{TKO\text{-}Ph}$HA78sc$_{SEC}$, and $^{wt\text{-}P35S}$HA78sc$_{SEC}$ purified from leaves) carry the expected complex *N*-glycans, indicating efficient secretion via the Golgi apparatus, where these modifications occur. Intensive labeling of the extracellular space and the Golgi found in our IEM studies confirms this assumption. The complete absence of plant-specific β-1,2-Xyl and α-1,2-Fuc on the HA78 scFv-Fc expressed in the *N*-glycosylation mutant TKO ($^{TKO\text{-}Ph}$HA78sc$_{SEC}$) confirms the suitability of this expression host for the production of glycoproteins with a humanized *N*-glycosylation profile. This is in accordance with our previous studies, where glyco-engineered Arabidopsis served as an expression system for the generation of mAbs with a humanized *N*-glycosylation profile (Strasser et al., 2004; Schähs et al., 2007; Loos et al., 2011). Glycan structures as obtained in these studies (i.e. GnGn structures) have been shown to enhance Fc-mediated effector functions of mAbs and thus may contribute to the development of pharmaceuticals with enhanced in vivo efficacy (Forthal et al., 2010).

An unexpected observation was the presence of substantial portions of oligomannosidic *N*-glycans on β-phaseolin-driven secretory HA78 scFv-Fcs. Such ER-typical glycans were hardly found on leaf-produced HA78 scFv-Fc ($^{wt\text{-}35S}$HA78sc$_{SEC}$ purified from leaf). This observation seems to be due to the special characteristics of the seed secretory system rather than a consequence of the substantially increased accumulation level of the β-phaseolin-driven constructs, as degradation products of 35S-driven secretory HA78 scFv-Fcs ($^{wt\text{-}35S}$HA78sc$_{SEC}$) purified from seeds also carry a substantial portion of oligomannosidic structures besides complex *N*-glycans (Supplemental Figs. S5 and S6; Supplemental Table S1). However, this increased fraction of ER-typical, oligomannosidic *N*-glycans is in line with the deposition pattern in mature seeds, where $^{wt\text{-}Ph}$HA78sc$_{SEC}$ is secreted to the extracellular space but is also partially deposited intracellularly in ER-derived structures (Supplemental Fig. S1). This partial retention, which is not found in developing seeds, might occur in an advanced developmental stage. Overloading of the translocation machinery, the onset of senescence, and, related to that, decreased translocation activity or a development-related switch in pathways can all be envisaged to explain this unusual phenomenon. The same difference between immature and mature seeds (i.e. a stronger tendency toward ER-derived structures in later stages of maturation) was also observed in maize (*Zea mays*) seeds expressing a recombinant protein (Arcalis et al., 2010).

Recently, full-length versions of 2G12 expressed in maize seeds and tobacco (*Nicotiana tabacum*) seeds have been shown to carry a substantial fraction of single GlcNAc residues (Rademacher et al., 2008; Ramessar et al., 2008; Floss et al., 2009). With the exception of some degradation products of 35S-driven HA78 scFv-Fc, this specific glycoform has not been found in this study or in related studies on the expression of antibodies or fragments in Arabidopsis seeds (Van Droogenbroeck et al., 2007; Loos et al., 2011), nor has it been reported upon expression of other mAbs in other plant seeds.

To our knowledge, our results represent the first study that examines in a systematic way the stability, subcellular targeting, and deposition of recombinantly expressed proteins in combination with a detailed monitoring of the *N*-glycosylation status. This important posttranslational modification occurs along the secretory pathway and allows conclusions on the subcellular trafficking of the target protein. In summary, we demonstrate the efficient expression of recombinant proteins in Arabidopsis seeds, the targeted subcellular deposition, and the generation of customized *N*-glycosylation patterns. These results emphasize the high potential of plant seeds as reliable and versatile expression hosts for the production of complex mammalian glycoproteins. However, we also reveal some unusual phenomena within the secretory pathway of transgenic seeds, like the formation of ER-derived vesicles upon the expression of recombinant proteins. The exact mechanism that initiates the formation of such vesicles is not yet fully understood. Further studies are required to elucidate intracellular trafficking mechanisms in seeds, which are of particular importance for the production of proteins that need special posttranslational modifications, like glycosylation, to obtain full biological activity. So far, this elucidation remains a case-to-case study.

MATERIALS AND METHODS

Cloning and Plant Transformation

2G12 V_H and V_L were amplified with forward primers containing *Sfi*I and *Apa*LI sites, respectively, and reverse primers containing *Xho*I and *Not*I sites, respectively. The fragments were cloned into the pHEN2 phagemid vector

(Van Droogenbroeck et al., 2007); from there, the scFv was excised via *Sfi*I and *Not*I sites and cloned in frame into pPICZαB (Invitrogen) containing a short linker fragment and the hinge-C_H2-C_H3 domains of the full-length 2G12 antibody, thereby constructing the 2G12 scFv-Fc. HA78 scFv-Fc was amplified from a scFv-Fc clone described previously (Van Droogenbroeck et al., 2007) with changes in the 5′ and 3′ ends to be the same as in the full-length HA78 construct (Loos et al., 2011) and to comply with the Kabat catalog.

The signal peptide of the 2S2 albumin of Arabidopsis (*Arabidopsis thaliana*) as well as the attB sites necessary for Gateway cloning were added by PCR to the scFv-Fcs. Both constructs were cloned with and without C-terminal addition of KDEL at the 3′ end before the stop codon. The four constructs were inserted via Gateway cloning (via an intermediate step in a pDONR clone) into the binary plant destination vector pPhasGW (F. Morandini, B. Van Droogenbroeck, A. Depicker, unpublished data) that allows high-level seed-specific expression.

Additionally, the secretory version of both scFv-Fcs were PCR amplified from the pDONR clones, and *Xba*I and *Bgl*II sites were added 5′ of the 2S2 signal peptide and 3′ of the stop codon, respectively. The fragments were cloned into the *Xba*I and *Bam*HI sites of the binary plant vector pPT2 (Strasser et al., 2005), where they are under the control of the cauliflower mosaic virus 35S promoter, allowing systemic expression in plants.

Arabidopsis wild-type plants were transformed by floral dip with all six constructs, and Arabidopsis TKO plants (Strasser et al., 2004) were transformed by the same method with the pPhasGW vector containing the secretory versions. Altogether, eight combinations of vector and genetic background were established (Table I).

Transgenic plants were selected on kanamycin containing Murashige and Skoog (Duchefa Biochemie) plant medium plates. The expression level was controlled by sandwich ELISA (coated, goat anti-human IgG [γ-chain], Sigma catalog no. I-7883; detected, goat anti-human IgG [γ-chain] conjugated to alkaline phosphatase, Sigma, catalog no. A-3187) and confirmed by immunoblotting against the heavy chain. Two lines each were taken to the homozygous state.

Protein Extraction from Leaves

Leaf material was weighed into 2-mL safe-lock, round-bottom Eppendorf tubes, two steel balls (5 mm) were added, and the tubes were frozen in liquid nitrogen and crushed in a ball mill (1 min, 70^{-s}). For every 1 mg of leaf material, 10 μL of extraction buffer (40 mM ascorbic acid, 500 mM NaCl, 1 mM EDTA, 45 mM Tris, pH 6.8, with HCl) was added, the samples were incubated for 15 min on ice and centrifuged for 5 min at maximum speed (tabletop centrifuge), and the supernatant was taken off.

Protein Extraction from Seeds and Antibody Purification

Five to 10 mg of seeds and two steel balls were added to appropriate reaction tubes, frozen in liquid nitrogen, and crushed in a ball mill. Fatty components were extracted with 950 μL of hexane. After 5 min of centrifugation at 10,000*g*, the supernatant was discarded and the samples were vacuum dried. Freezing, crushing, hexane extraction, and drying were repeated, and the pellets were completely resuspended in 900 μL of ice-cold extraction buffer (40 mM ascorbic acid, 500 mM NaCl, 1 mM EDTA, 45 mM Tris, pH 6.8, with HCl) and incubated on ice for 15 min. The insoluble material was removed by centrifugation in a tabletop centrifuge at 20,000*g* (4°C) for 5 min. The supernatant was kept on ice while the extraction procedure was repeated. The supernatants were pooled, centrifuged at 35,000*g* (4°C) for 30 min, and filtered through a 2.5-μm filter. The centrifugation was repeated, and the cleared extract was filtered through a 0.45-μm filter. The filtrate was then applied to a column packed with 1 mL of Protein A Fast Flow Sepharose (GE Healthcare). scFv-Fcs were eluted with 100 mM Gly, pH 3.0, and immediately neutralized with 500 mM Tris, pH 8.0. $^{wt\text{-}35S}$HA78sc_{SEC} purified from seeds was concentrated via an additional Protein A purification step described below.

Purification of scFv-Fcs Expressed under the Control of the 35S Promoter

Leaf extracts of 200 μL or approximately 1 mL of $^{wt\text{-}35S}$HA78sc_{SEC} purified from seeds as described above were mixed with 25 μL of washed Protein A-Sepharose (GE Healthcare catalog no. 17-1279-01) and shaken at 4°C for 120 min. The beads were centrifuged for 5 min at 5,000 rpm (tabletop centrifuge), the supernatant was discarded, and the beads were resuspended in 750 μL of PBST (phosphate-buffered saline [PBS] and 0.1% [v/v] Tween 20) and transferred to a column (Micro Bio-Spin Chromatography Column; Bio-Rad catalog no. 732-6204). The beads were washed at least twice with 700 μL of PBS. Thirty-five microliters of 1× Laemmli loading buffer was added, and the column was sealed, heated for 3 min at 96°C, and centrifuged for 1 min at 1,000g. The flow-through was reapplied and heating and centrifugation were repeated.

N-Glycan Analysis

N-Glycan analysis was carried out by LC-electrospray ionization (ESI)-MS of tryptic glycopeptides (Stadlmann et al., 2008). In short, the scFv-Fc bands of Coomassie Brilliant Blue-stained SDS-PAGE gels were excised, protein S alkylated, digested with trypsin, and subsequently analyzed by LC-ESI-MS. Due to incomplete tryptic digest, each glycan structure is represented by two glycopeptides that differ by 482 D (glycopeptide 1, EEQYNSTYR; glycopeptide 2, TKPREEQYNSTYR).

For Man7 isomer analysis, *N*-glycans were released by peptide:*N*-glycosidase A or F and purified by passage over a reverse-phase cartridge followed by borohydride reduction and purification over a graphitic carbon cartridge as described previously (Stadlmann et al., 2008). The reduced oligosaccharides were separated on a capillary porous graphitic carbon column and detected by LC-ESI-MS (Pabst et al., 2007). Oligomannosidic reference glycans were prepared from *Phaseolus vulgaris* in a similar manner. Their structure is known from previous NMR analyses (Neeser et al., 1985). The assignments of these reference glycans were corroborated by parallel analysis of 2-aminopyridine-labeled glycans (Tomiya et al., 1991; Liebminger et al., 2009).

Antigen-Binding Activity of Purified scFv-Fcs

Antigen-binding activity was determined by ELISA as described previously (Van Droogenbroeck et al., 2007; Strasser et al., 2008). For HA78 scFv-Fcs, microtiter plates were coated overnight at 4°C with hepatitis A antigen diluted in coating buffer (0.05 M sodium carbonate buffer, pH 9.6). After washing four times, the plates were blocked with 2% skim milk in PBS. One hundred microliters of the purified antibody preparations was added per well in a 2-fold dilution series beginning with 0.5 μg mL^{-1} and incubated at 37°C for 1.5 h. Wells were washed and incubated with horseradish peroxidase (HRP)-conjugated anti-human IgG Fc (Sigma) antibodies followed by tetramethylbenzidine for development. PBS was used as a negative control. For 2G12 scFv-Fcs, ELISA plates were coated with 100 ng of purified gp120. After washing, 50 μL of a 1:2 serial dilution of the 2G12 scFv-Fc was added per well. As a standard, recombinant 2G12 purified from CHO culture supernatants was used. Plates were incubated for 1 h at room temperature (gentle shaking), and after washing, the wells were incubated with a goat anti-human IgG (κ chain) polyclonal antibody conjugated to alkaline phosphatase (1:1,000; Sigma). After intensive washing, alkaline phosphatase was detected by *p*-nitro-phenylphosphate.

Virus Neutralization Assays

$^{wt\text{-}Ph}$2G12sc_{KDEL} was tested with an syncytium inhibition assay as described previously (Purtscher et al., 1994) for HIV neutralization efficiency. As the other 2G12 constructs displayed the same *N*-glycosylation profile, they were not tested. In brief, after preincubating a dilution series of scFv-Fcs with HIV, CD4-positive human AA-2 cells were added. Five days later, the presence of at least one syncytium was evaluated as positive and the antibody concentration was calculated, at which 50% inhibition of the initial syncytium-forming activity was observed (IC_{50}; Reed, 1938). The assays were performed in duplicate.

Hepatitis A virus neutralization was tested as described previously (MacGregor et al., 1983; Van Droogenbroeck et al., 2007). Then, HepA virus strain JN was preincubated with a dilution series of purified scFv-Fcs (Gao, 1989), after which appropriate virus target cells (FRhK-4) were infected. Hepatitis A infection was determined after 21 d of incubation by ELISA with human anti-HepA polyclonal antibody as coating antibody and HRP-conjugated anti-HepA mAb from mouse for detection. Neutralization efficiencies were calculated according to the method of Reed (1938).

IEM

IEM on developing seeds was performed as described previously (Loos et al., 2011). Briefly, developing embryos were high-pressure frozen, freeze substituted with acetone, and infiltrated with HM20. Polymerization was conducted with UV light at −35°C. Sections were labeled with γ-chain-specific antibodies and secondary gold-coupled antibodies. After postcontrasting, the samples were analyzed with a JEOL JEM-1400 transmission electron microscope at 80 kV. IEM on mature seeds was performed as described in Supplemental Materials and Methods S1.

Supplemental Data

The following materials are available in the online version of this article.

Supplemental Figure S1. Subcellular localization of $^{wt\text{-}Ph}$HA78sc$_{SEC}$ in mature Arabidopsis seeds by immunogold electron microscopy.

Supplemental Figure S2. Subcellular localization of $^{wt\text{-}Ph}$HA78sc$_{KDEL}$ in mature Arabidopsis seeds by immunogold electron microscopy.

Supplemental Figure S3. Subcellular localization of $^{wt\text{-}Ph}$2G12sc$_{SEC}$ in mature Arabidopsis seeds by immunogold electron microscopy.

Supplemental Figure S4. Subcellular localization of $^{wt\text{-}Ph}$2G12sc$_{KDEL}$ in mature Arabidopsis seeds by immunogold electron microscopy.

Supplemental Figure S5. Coomassie-stained SDS-PAGE of $^{wt\text{-}35S}$HA78sc$_{SEC}$ purified from seeds.

Supplemental Figure S6. *N*-glycosylation pattern of the degradation products of seed-produced ^{wt_35S}HA78sc$_{SEC}$.

Supplemental Table S1. Relative distribution of *N*-glycans of the degraded fragments of seed-extracted $^{wt\text{-}35S}$HA78sc$_{SEC}$, $^{wt\text{-}Ph}$HA78sc$_{SEC}$, and $^{TKO\text{-}Ph}$HA78sc$_{SEC}$.

Supplemental Materials and Methods S1. IEM of mature seeds.

Supplemental Results S1. Subcellular localization in mature seeds and N-glycosylation of degradation products.

ACKNOWLEDGMENTS

We thank Mohammad-Ali Assadian-Tschalschotori (Polymun Scientific, Vienna) for 2G12 quantification and Pia Gattinger, Jakub Jez, and Julian Rodriguez (University of Natural Resources and Applied Life Sciences), Els Van Lerberge (Department of Plant Systems Biology, Flanders Institute for Biotechnology, Ghent University), and Steffi Gold (Heidelberg Institute for Plant Sciences, University of Heidelberg) for indispensable technical help.

Received December 27, 2010; accepted February 11, 2011; published February 16, 2011.

LITERATURE CITED

Abranches R, Arcalis E, Marcel S, Altmann F, Ribeiro-Pedro M, Rodriguez J, Stoger E (2008) Functional specialization of Medicago truncatula leaves and seeds does not affect the subcellular localization of a recombinant protein. Planta **227:** 649–658

Aggarwal S (2009) What's fueling the biotech engine: 2008. Nat Biotechnol **27:** 987–993

Arcalis E, Stadlmann J, Marcel S, Drakakaki G, Winter V, Rodriguez J, Fischer R, Altmann F, Stoger E (2010) The changing fate of a secretory glycoprotein in developing maize endosperm. Plant Physiol **153:** 693–702

Boothe J, Nykiforuk C, Shen Y, Zaplachinski S, Szarka S, Kuhlman P, Murray E, Morck D, Moloney MM (2010) Seed-based expression systems for plant molecular farming. Plant Biotechnol J **8:** 588–606

Calarese DA, Scanlan CN, Zwick MB, Deechongkit S, Mimura Y, Kunert R, Zhu P, Wormald MR, Stanfield RL, Roux KH, et al (2003) Antibody domain exchange is an immunological solution to carbohydrate cluster recognition. Science **300:** 2065–2071

Cao J, Meng S, Li C, Ji Y, Meng Q, Zhang Q, Liu F, Li J, Bi S, Li D, et al (2008) Efficient neutralizing activity of cocktailed recombinant human antibodies against hepatitis A virus infection in vitro and in vivo. J Med Virol **80:** 1171–1180

Cao M, Cao P, Yan HJ, Lu WG, Ren F, Hu YL, Zhang SQ (2009) Construction, purification, and characterization of anti-BAFF scFv-Fc fusion antibody expressed in CHO/dhfr- cells. Appl Biochem Biotechnol **157:** 562–574

Clerc S, Hirsch C, Oggier DM, Deprez P, Jakob C, Sommer T, Aebi M (2009) Htm1 protein generates the N-glycan signal for glycoprotein degradation in the endoplasmic reticulum. J Cell Biol **184:** 159–172

De Jaeger G, Scheffer S, Jacobs A, Zambre M, Zobell O, Goossens A, Depicker A, Angenon G (2002) Boosting heterologous protein production in transgenic dicotyledonous seeds using Phaseolus vulgaris regulatory sequences. Nat Biotechnol **20:** 1265–1268

De Lorenzo C, D'Alessio G (2009) Human anti-ErbB2 immunoagents: immunoRNases and compact antibodies. FEBS J **276:** 1527–1535

Dhaese P, De Greve H, Gielen J, Seurinck L, Van Montagu M, Schell J (1983) Identification of sequences involved in the polyadenylation of higher plant nuclear transcripts using Agrobacterium T-DNA genes as models. EMBO J **2:** 419–426

Downing WL, Galpin JD, Clemens S, Lauzon SM, Samuels AL, Pidkowich MS, Clarke LA, Kermode AR (2006) Synthesis of enzymatically active human alpha-L-iduronidase in Arabidopsis cgl (complex glycan-deficient) seeds. Plant Biotechnol J **4:** 169–181

Fiedler U, Conrad U (1995) High-level production and long-term storage of engineered antibodies in transgenic tobacco seeds. Biotechnology (N Y) **13:** 1090–1093

Fiedler U, Phillips J, Artsaenko O, Conrad U (1997) Optimization of scFv antibody production in transgenic plants. Immunotechnology **3:** 205–216

Filpula D (2007) Antibody engineering and modification technologies. Biomol Eng **24:** 201–215

Floss DM, Sack M, Arcalis E, Stadlmann J, Quendler H, Rademacher T, Stoger E, Scheller J, Fischer R, Conrad U (2009) Influence of elastin-like peptide fusions on the quantity and quality of a tobacco-derived human immunodeficiency virus-neutralizing antibody. Plant Biotechnol J **7:** 899–913

Forthal DN, Gach JS, Landucci G, Jez J, Strasser R, Kunert R, Steinkellner H (2010) Fc-glycosylation influences Fcγ receptor binding and cell-mediated anti-HIV activity of monoclonal antibody 2G12. J Immunol **185:** 6876–6882

Gao F (1989) Expression of hepatitis A virus proteins by recombinant vaccinia virus. Chin J Virol **5:** 303–311

Geyer BC, Kannan L, Cherni I, Woods RR, Soreq H, Mor TS (2010) Transgenic plants as a source for the bioscavenging enzyme, human butyrylcholinesterase. Plant Biotechnol J **8:** 873–886

Harmsen MM, De Haard HJ (2007) Properties, production, and applications of camelid single-domain antibody fragments. Appl Microbiol Biotechnol **77:** 13–22

Herman EM, Tague BW, Hoffman LM, Kjemtrup SE, Chrispeels MJ (1990) Retention of phytohemagglutinin with carboxyterminal tetrapeptide KDEL in the nuclear envelope and the endoplasmatic reticulum. Planta **182:** 305–312

Invitrogen (2003) Gateway technology: a universal technology to clone DNA sequences for functional analysis and expression in multiple systems. http://tools.invitrogen.com/content/sfs/manuals/gatewayman.pdf (September 22, 2003)

Islam MR, Kung S-S, Kimura Y, Funatsu G (1991) N-Acetyl-D-glucosamine-asparagine structure in ribosome-inactivating proteins from the seeds of *Luffa cylindrica* and *Phytolacca americana*. Agric Biol Chem **55:** 1375–1381

Ko K, Steplewski Z, Glogowska M, Koprowski H (2005) Inhibition of tumor growth by plant-derived mAb. Proc Natl Acad Sci USA **102:** 7026–7030

Krebbers E, Herdies L, De Clercq A, Seurinck J, Leemans J, Van Damme J, Segura M, Gheysen G, Van Montagu M, Vandekerckhove J (1988) Determination of the processing sites of an Arabidopsis 2S albumin and characterization of the complete gene family. Plant Physiol **87:** 859–866

Laguía-Becher M, Martín V, Kraemer M, Corigliano M, Yacono ML, Goldman A, Clemente M (2010) Effect of codon optimization and subcellular targeting on Toxoplasma gondii antigen SAG1 expression in tobacco leaves to use in subcutaneous and oral immunization in mice. BMC Biotechnol **10:** 52

Li SL, Liang SJ, Guo N, Wu AM, Fujita-Yamaguchi Y (2000) Single-chain antibodies against human insulin-like growth factor I receptor: expres-

sion, purification, and effect on tumor growth. Cancer Immunol Immunother **49:** 243–252

Liebminger E, Hüttner S, Vavra U, Fischl R, Schoberer J, Grass J, Blaukopf C, Seifert GJ, Altmann F, Mach L, et al (2009) Class I α-mannosidases are required for *N*-glycan processing and root development in *Arabidopsis thaliana*. Plant Cell **21:** 3850–3867

Liebminger E, Veit C, Mach L, Strasser R (2010) Mannose trimming reactions in the early stages of the N-glycan processing pathway. Plant Signal Behav **5:** 476–478

Loos A, Van Droogenbroeck B, Hillmer S, Grass J, Kunert R, Cao J, Robinson DG, Depicker A, Steinkellner H (2011) Production of monoclonal antibodies with a controlled N-glycosylation pattern in seeds of Arabidopsis thaliana. Plant Biotechnol J **9:** 179–192

MacGregor A, Kornitschuk M, Hurrell JG, Lehmann NI, Coulepis AG, Locarnini SA, Gust ID (1983) Monoclonal antibodies against hepatitis A virus. J Clin Microbiol **18:** 1237–1243

Moravec T, Schmidt MA, Herman EM, Woodford-Thomas T (2007) Production of Escherichia coli heat labile toxin (LT) B subunit in soybean seed and analysis of its immunogenicity as an oral vaccine. Vaccine **25:** 1647–1657

Mori K, Kim YU (2008) Molecular cloning and characterization of a single-chain variable fragment antibody specific for benzoylecgonine expressed in Escherichia coli. J Microbiol **46:** 571–578

Müntz K (1998) Deposition of storage proteins. Plant Mol Biol **38:** 77–99

Neeser J-R, Del Vedovo S, Mutsaers JHGM, Vliegenthart JFG (1985) Structural analysis of the carbohydrate chains of legume storage proteins by 500-MHz ^{1}H-NMR spectroscopy. Glycoconj J **2:** 355–364

Olafsen T, Betting D, Kenanova VE, Salazar FB, Clarke P, Said J, Raubitschek AA, Timmerman JM, Wu AM (2009) Recombinant anti-CD20 antibody fragments for small-animal PET imaging of B-cell lymphomas. J Nucl Med **50:** 1500–1508

Pabst M, Bondili JS, Stadlmann J, Mach L, Altmann F (2007) Mass + retention time = structure: a strategy for the analysis of N-glycans by carbon LC-ESI-MS and its application to fibrin N-glycans. Anal Chem **79:** 5051–5057

Petruccelli S, Otegui MS, Lareu F, Tran Dinh O, Fitchette AC, Circosta A, Rumbo M, Bardor M, Carcamo R, Gomord V, et al (2006) A KDEL-tagged monoclonal antibody is efficiently retained in the endoplasmic reticulum in leaves, but is both partially secreted and sorted to protein storage vacuoles in seeds. Plant Biotechnol J **4:** 511–527

Philip R, Darnowski DW, Maughan PJ, Vodkin LO (2001) Processing and localization of bovine beta-casein expressed in transgenic soybean seeds under control of a soybean lectin expression cassette. Plant Sci **161:** 323–335

Philip R, Darnowski DW, Sundararaman V, Cho MJ, Vodkin LO (1998) Localization of beta-glucuronidase in protein bodies of transgenic tobacco seed by fusion to an amino terminal sequence of the soybean lectin gene. Plant Sci **137:** 191–204

Powers DB, Amersdorfer P, Poul MA, Nielsen UB, Shalaby MR, Adams GP, Weiner LM, Marks JD (2001) Expression of single-chain Fv-Fc fusions in Pichia pastoris. J Immunol Methods **251:** 123–135

Purtscher M, Trkola A, Gruber G, Buchacher A, Predl R, Steindl F, Tauer C, Berger R, Barrett N, Jungbauer A, et al (1994) A broadly neutralizing human monoclonal antibody against gp41 of human immunodeficiency virus type 1. AIDS Res Hum Retroviruses **10:** 1651–1658

Rademacher T, Sack M, Arcalis E, Stadlmann J, Balzer S, Altmann F, Quendler H, Stiegler G, Kunert R, Fischer R, et al (2008) Recombinant antibody 2G12 produced in maize endosperm efficiently neutralizes HIV-1 and contains predominantly single-GlcNAc N-glycans. Plant Biotechnol J **6:** 189–201

Raju TS (2008) Terminal sugars of Fc glycans influence antibody effector functions of IgGs. Curr Opin Immunol **20:** 471–478

Ramessar K, Rademacher T, Sack M, Stadlmann J, Platis D, Stiegler G, Labrou N, Altmann F, Ma J, Stöger E, et al (2008) Cost-effective production of a vaginal protein microbicide to prevent HIV transmission. Proc Natl Acad Sci USA **105:** 3727–3732

Reed LJMIL (1938) A simple method for estimating fifty percent endpoints. Am J Hyg **27:** 493–497

Reggi S, Marchetti S, Patti T, De Amicis F, Cariati R, Bembi B, Fogher C (2005) Recombinant human acid β-glucosidase stored in tobacco seed is stable, active and taken up by human fibroblasts. Plant Mol Biol **57:** 101–113

Riccio G, Esposito G, Leoncini E, Contu R, Condorelli G, Chiariello M, Laccetti P, Hrelia S, D'Alessio G, De Lorenzo C (2009) Cardiotoxic effects, or lack thereof, of anti-ErbB2 immunoagents. FASEB J **23:** 3171–3178

Robinson DG, Oliviusson P, Hinz G (2005) Protein sorting to the storage vacuoles of plants: a critical appraisal. Traffic **6:** 615–625

Schähs M, Strasser R, Stadlmann J, Kunert R, Rademacher T, Steinkellner H (2007) Production of a monoclonal antibody in plants with a humanized N-glycosylation pattern. Plant Biotechnol J **5:** 657–663

Schmidt MA, Herman EM (2008) Proteome rebalancing in soybean seeds can be exploited to enhance foreign protein accumulation. Plant Biotechnol J **6:** 832–842

Schouten A, Roosien J, van Engelen FA, de Jong GAM, Borst-Vrenssen AW, Zilverentant JF, Bosch D, Stiekema WJ, Gommers FJ, Schots A, et al (1996) The C-terminal KDEL sequence increases the expression level of a single-chain antibody designed to be targeted to both the cytosol and the secretory pathway in transgenic tobacco. Plant Mol Biol **30:** 781–793

Shu L, Qi CF, Schlom J, Kashmiri SV (1993) Secretion of a single-gene-encoded immunoglobulin from myeloma cells. Proc Natl Acad Sci USA **90:** 7995–7999

Stadlmann J, Pabst M, Kolarich D, Kunert R, Altmann F (2008) Analysis of immunoglobulin glycosylation by LC-ESI-MS of glycopeptides and oligosaccharides. Proteomics **8:** 2858–2871

Stoger E, Sack M, Perrin Y, Vaquero C, Torres E, Twyman RM, Christou P, Fischer R (2002) Practical considerations for pharmaceutical antibody production in different crop systems. Mol Breed **9:** 149–158

Strasser R, Altmann F, Mach L, Glössl J, Steinkellner H (2004) Generation of Arabidopsis thaliana plants with complex N-glycans lacking beta1,2-linked xylose and core alpha1,3-linked fucose. FEBS Lett **561:** 132–136

Strasser R, Stadlmann J, Schähs M, Stiegler G, Quendler H, Mach L, Glössl J, Weterings K, Pabst M, Steinkellner H (2008) Generation of glyco-engineered Nicotiana benthamiana for the production of monoclonal antibodies with a homogeneous human-like N-glycan structure. Plant Biotechnol J **6:** 392–402

Strasser R, Stadlmann J, Svoboda B, Altmann F, Glössl J, Mach L (2005) Molecular basis of N-acetylglucosaminyltransferase I deficiency in Arabidopsis thaliana plants lacking complex N-glycans. Biochem J **387:** 385–391

Takaiwa F, Katsube T, Kitagawa S, Hisago T, Kito M, Utsumi S (1995) High level accumulation of soybean glycinin in vacuole-derived protein bodies in the endosperm tissue of transgenic tobacco seed. Plant Sci **111:** 39–49

Tomiya N, Lee YC, Yoshida T, Wada Y, Awaya J, Kurono M, Takahashi N (1991) Calculated two-dimensional sugar map of pyridylaminated oligosaccharides: elucidation of the jack bean alpha-mannosidase digestion pathway of Man9GlcNAc2. Anal Biochem **193:** 90–100

Trkola A, Purtscher M, Muster T, Ballaun C, Buchacher A, Sullivan N, Srinivasan K, Sodroski J, Moore JP, Katinger H (1996) Human monoclonal antibody 2G12 defines a distinctive neutralization epitope on the gp120 glycoprotein of human immunodeficiency virus type 1. J Virol **70:** 1100–1108

Van Droogenbroeck B, Cao J, Stadlmann J, Altmann F, Colanesi S, Hillmer S, Robinson DG, Van Lerberge E, Terryn N, Van Montagu M, et al (2007) Aberrant localization and underglycosylation of highly accumulating single-chain Fv-Fc antibodies in transgenic Arabidopsis seeds. Proc Natl Acad Sci USA **104:** 1430–1435

Wandelt CI, Khan MR, Craig S, Schroeder HE, Spencer D, Higgins TJ (1992) Vicilin with carboxy-terminal KDEL is retained in the endoplasmic reticulum and accumulates to high levels in the leaves of transgenic plants. Plant J **2:** 181–192

Wright KE, Prior F, Sardana R, Altosaar I, Dudani AK, Ganz PR, Tackaberry ES (2001) Sorting of glycoprotein B from human cytomegalovirus to protein storage vesicles in seeds of transgenic tobacco. Transgenic Res **10:** 177–181

Yuan QA, Simmons HH, Robinson MK, Russeva M, Marasco WA, Adams GP (2006) Development of engineered antibodies specific for the Müllerian inhibiting substance type II receptor: a promising candidate for targeted therapy of ovarian cancer. Mol Cancer Ther **5:** 2096–2105

Zeng Z-H, He X-L, Li H-M, Hu Z, Wang D-C (2003) Crystal structure of pokeweed antiviral protein with well-defined sugars from seeds at 1.8A resolution. J Struct Biol **141:** 171–178

Zhang W, Matsumoto-Takasaki A, Kusada Y, Sakaue H, Sakai K, Nakata M, Fujita-Yamaguchi Y (2007) Isolation and characterization of phage-displayed single chain antibodies recognizing nonreducing terminal mannose residues. 2. Expression, purification, and characterization of recombinant single chain antibodies. Biochemistry **46:** 263–270